Geological setting and concentration of scandium in the Flatreef and eastern limb chromitites of the Bushveld Complex

by E. Kotze[1], F. Roelofse[1], D. Grobler[2], C. Gauert[3], and M. Purchase[1]

Affiliation:
[1]University of the Free State, South Africa.
[2]Ivanhoe Mines Ltd.
[3]Dezernat für Angewandte Geologie und Georisiken, Landesamt für Geologie und Bergwesen Sachsen-Anhalt.

Correspondence to:
E. Kotze

Email:
kotze.e@ufs.ac.za

Dates:
Received: 17 Jan. 2022
Revised: 29 May 2022
Accepted: 8 Jun. 2022
Published: September 2022

How to cite:
Kotze, E., Roelofse, F., Grobler, D., Gauert, C., and Purchase, M. 2022 Geological setting and concentration of scandium in the Flatreef and eastern limb chromitites of the Bushveld Complex.
Journal of the Southern African Institute of Mining and Metallurgy, vol. 122, no. 9, pp. 517–526

DOI ID:
http://dx.doi.org/10.17159/2411-9717/1987/2022

ORCID:
E. Kotze
https://orcid.org/0000-0003-3195-713

Synopsis

Scandium is an important industrial metal for which demand is projected to increase in the future. Although many Sc deposits are secondary, Sc is scavenged by clinopyroxene during fractional crystallization of primary, mafic-ultramafic magmas. Sc may thus occur in sub-economic concentrations in mafic-ultramafic intrusions. In this work, we present new data on the concentration of Sc in the Bushveld Complex (BC) of South Africa. The eastern and western limbs of the BC are considered to be largely pristine, primary magmatic deposits, whereas the northern limb shows evidence of large-scale, localized crustal contamination. Samples from the primary magmatic cumulates of the eastern limb, from the mineralized Flatreef of the northern limb, and from the crustal-contaminated Footwall Assimilation Zone (FAZ) of the Flatreef were analysed for Sc. Despite the FAZ containing abundant clinopyroxene, interpreted to have recrystallized from the original cumulates in the presence of melted sedimentary rocks, no significant differences are seen in the concentration of Sc compared to other cumulate rocks of the BC containing less-abundant clinopyroxene. The concentration of Sc in the analysed samples is mainly controlled by mineralogy, with anorthosites, chromitites, and harzburgites containing under 20 ppm, and norites and pyroxenites containing 20–40 ppm. The parapyroxenites of the FAZ are less enriched in Sc than expected, suggesting that Sc may have been lost during alteration and recrystallization.

Keywords

scandium, Flatreef, Bushveld Complex, rare earth elements, igneous processes.

Introduction

The Bushveld Complex (BC) (Figure 1), which is located in the north of South Africa, is a gigantic assemblage of intrusive magmatic and associated rocks (*e.g.* Willemse, 1966) estimated to be 2.055 billion years old (Zeh *et al.*, 2015). The mafic to ultramafic phase of the BC is termed the Rustenburg Layered Suite (RLS) (Willemse, 1966; Cawthorn and Webb, 2001; Cawthorn *et al.*, 2006; Kruger, 2005). Associated with the RLS are the later acid suites (the Lebowa Granite and Rashoop Granophyre suites) (Von Gruenewaldt, Sharpe, and Hatton, 1985; Van Tongeren, Mathez, and Kelemen, 2010), as well as smaller intrusive bodies (sills, dykes and magmatic pipes) (*e.g.* Tarkian and Stumpfl, 1975; Harmer and Sharpe, 1985; Viljoen and Scoon, 1985; Scoon and Mitchell, 1994; 2004).

The BC boasts many different types of economic mineralization. It is the world's largest single repository of the six platinum group elements (PGE) (*e.g.* Cawthorn *et al.*, 2002; Arndt *et al.*, 2005), with the pyroxenitic Merensky Reef accounting for much of the PGE production (*e.g.* Cousins, 1966; Lee, 1996; Cawthorn *et al.*, 2002). Also closely associated with the PGE are the laterally continuous chromitite layers (*e.g.* Von Gruenewaldt, Hatton, and Merkle *et al.*, 1986; Lee and Parry, 1988; Kinnaird *et al.*, 2002; Oberthür *et al.*, 2015), a major source of the world's chromium (*e.g.* Cameron & Desborough, 1966; Teigler and Eales, 1993; Cawthorn *et al.*, 2006). Grades of PGE in the chromitite layers range from below 0.5 ppm up to 10 ppm in the UG-2 chromitite (Von Gruenewaldt *et al.*, 1986; Lee & Parry, 1988; Lee, 1996; Kinnaird *et al.*, 2002; Arndt *et al.*, 2005). The Main Magnetite Layer (MML) is exploited for vanadium (Cawthorn and Webb, 2001) and also hosts titanium resources that may be exploitable in the future (Cawthorn *et al.*, 2006; Harney and Von Gruenewaldt, 1995). The BC is also a source of the base metals Co, Cu and Ni, (*e.g.* Cramer, 2001; Jones, 2005) as well as gold, (*e.g.* Godel, Barnes, Maier, 2007; Van der Merwe, Viljoen, and Knoper *et al.*, 2012) all of which are closely associated with the PGE and are typically separated from them during mineral processing to be sold as secondary commodities (*e.g.* Jones, 2005; Jacobs, 2006). Tin has also been mined from intrusive pipes associated with the granites of the BC (Von Gruenewaldt and Strydom, 1985; Coetzee and Twist, 1989; Kinnaird and McDonald, 2005).

Geological setting and concentration of scandium

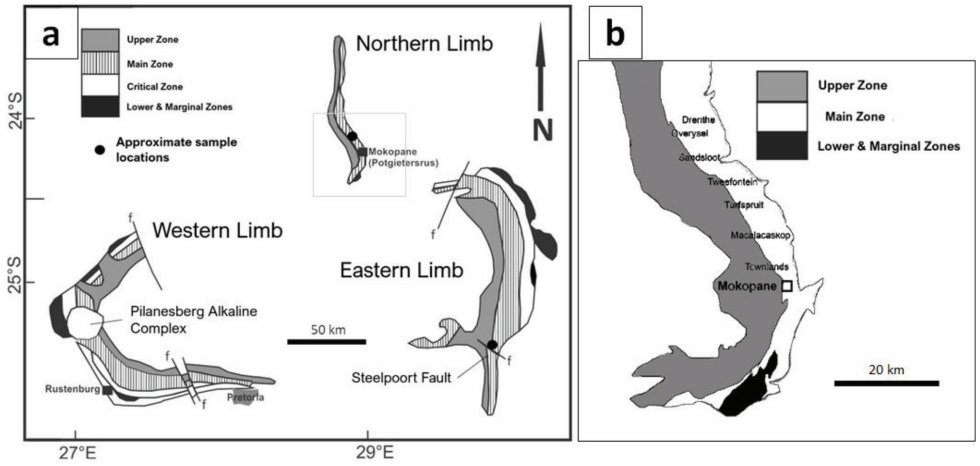

Figure 1—(a) The outcropping rocks of the Rustenburg Layered Suite of the BC, indicating the three main limbs (north, east and west) of the Complex. (b) Magnified view of the southern part of the northern limb where samples originated on the properties of Turfspruit and Macalacaskop (modified after Grobler *et al.*, 2019)

Despite all it has produced so far, the BC may still be host to metal and other commodities that have yet to be exploited.

Scandium

Due to its similar applications in industry, similar chemical properties, and occurrence alongside the lanthanides, scandium may be classified as one of the rare earth elements (REE) (Williams-Jones and Vasyukova, 2018; Wang *et al.*, 2021; Xie *et al.*, 2014). Sc concentrates are traded alongside REE concentrates, but most REE deposits are not significantly enriched in Sc (Williams-Jones and Vasyukova, 2018). However, Sc is mainly mined as a by-product from deposits that primarily exploit the other REE (Xiao *et al.*, 2020; Wang *et al.*, 2021).

Scandium is considered a valuable metal because of its uses in current technological developments. One of the main uses is to reduce the mass of aircraft and vehicles, which may be accomplished by substituting a lightweight, strong alloy of Sc and Al for other metals (Williams-Jones and Vasyukova, 2018; Hughes, Andersen, and Driscoll, 2021; Wang *et al.*, 2021). It is also used for solid oxide fuel cells (Hughes, Andersen, and Driscoll, 2021; European Commission, 2021; Wang *et al.*, 2021), which can be used to produce electricity on scales ranging from portable battery chargers to generators for fuel plants (Minh, 2004). Scandium is traded globally alongside the rare earth elements as well as 'minor' metals such tellurium, antimony, and bismuth (Shanghai Metals Market, 2022). According to the European Commission (2021), the main world producers of Sc are China, Russia, and the Ukraine, with China producing over two-thirds of the world's supply. With global events trending as they are, the Sc supply chain from Russia and the Ukraine is particularly at risk. Disruption of supply could result in shortages of all commodities supplied by these two countries, having wide-ranging effects on the various industries which rely upon them (*e.g.* Burke, 2022; Johnston, 2022; Kahn, 2022). In the case of Sc, these industries include the manufacture of semiconductors and batteries, as well as the aeronautics and renewable energy sectors.

Unlike the other REE, Sc is compatible with early rock-forming minerals. In the 3+ oxidation state, it may substitute for Mg and Fe in minerals such as pyroxene and amphibole (Williams-Jones and Vasyukova, 2018). Sc is known to be compatible with clinopyroxene during crystallization, but less compatible with orthopyroxene and incompatible with plagioclase and olivine (Allègre *et al.*, 1977; Morimoto *et al.*, 1988; Nielsen, Gallaham, and Newberger, 1992; Williams-Jones and Vasyukova, 2018). There exists a clinopyroxene that contains Sc as an essential element, namely jervisite ($NaScSi_2O_6$) (Hawthorne and Grundy, 1973; Morimoto *et al.*, 1988; Deer, Howie, Howie, and Zussman, 2013; Williams-Jones & Vasyukova, 2018). In the world's largest single resource of Sc, China's Bayan Obo deposit, Sc is found in aegirine of hydrothermal origin (Williams-Jones and Vasyukova, 2018). However, Sc may be found enriched in any of the clinopyroxenes associated with mafic-ultramafic intrusive deposits, such as augite and hedenbergite, where it may substitute for Mg or Fe in the M1-site (Morimoto *et al.*, 1988; Williams-Jones and Vasyukova, 2018; Wang *et al.*, 2021). The first stage of Sc enrichment in any deposit may be considered to be fractional crystallization, which produces Sc-enriched clinopyroxene in rocks of mafic to ultramafic composition (Wang *et al.*, 2021). Further stages of Sc enrichment may include hydrothermal activity, or surficial weathering in lateritic environments such as the bauxite deposits in Madagascar or Ni-Co laterites of New Caledonia (Taylor *et al.*, 2005; Williams-Jones and Vasyukova, 2018; Teitler *et al.*, 2019; Wang *et al.*, 2021). Lateritic Sc enrichment commonly occurs in iron oxide deposits overlying ultramafic intrusive pipes (Ural-Alaskan type intrusions), which is the case for the New Caledonian deposits (Teitler *et al.*, 2019) and for the Sunrise Ni-Co laterite of Australia, which is sporadically enriched in Pt as well as Sc (SRK Consulting, 2018).

The methods used to extract Sc are mainly hydrometallurgical (Xiao *et al.*, 2020). Like the other rare earth elements, Sc may be roasted to produce a concentrate which is then leached by acids such as HCl, HNO_3, and H_2SO_4 (Xie *et al.*, 2014). At Bayan Obo, Sc is extracted from tailings that have already been processed for Fe and the other REE (Williams-Jones and Vasyukova, 2018; Wang *et al.*, 2021). Aegirine at Bayan Obo is roasted before leaching to decompose it (Williams-Jones and Vasyukova, 2018). Scandium occurring in oxidized deposits such as Ni-Co laterites is particularly suited to hydrometallurgical extraction since it has already been weathered out of the silicates and occurs in oxide minerals such as goethite (Teitler *et al.*, 2019).

Since Sc is mainly produced as a by-product to other elements (Xiao *et al.*, 2020), cut-off grades vary considerably between operations. According to Williams-Jones and Vasyukova, (2018) the average grade of Sc in currently exploited as well as reserve

deposits across the world varies from 50–200 ppm. Teitler *et al.* (2019) consider high-grade lateritic Sc deposits to be those over 300 ppm, while those of 100 ppm and below are generally too low to be exploited, except for Sc as a by-product. Concentrations of Sc in pyroxenitic rocks of notable mafic-ultramafic intrusions such as the Russian Urals and similar intrusions in China range from 54 to 135 ppm (Wang *et al.*, 2021).

Although Sc is usually not significantly enriched in layered intrusions (Wang *et al.*, 2021), it is of both scientific and economic interest to investigate this element in the BC, particularly the ore-bearing horizons of the Flatreef and their footwalls, the latter being significantly contaminated with crustal material (Keir-Sage *et al.*, 2021; Maier *et al.*, 2021) and are not considered to represent a typical igneous BC cumulate.

The Flatreef

The northern limb (see Figure 1b) of the BC lacks the consistent and ubiquitous mineral layering of the RLS of the western and eastern limbs, although it does host PGE mineralization in a horizon of sulphide-bearing pyroxenite broadly similar to the Merensky Reef, which is known as the Platreef (Kinnaird and McDonald, 2005; Van der Merwe, Viljoen and Knoper, 2012). The Flatreef represents a thick, almost horizontal, laterally continuous down-dip extension of the Platreef (Hutchinson and Kinnaird, 2005; Maier *et al.*, 2021) which hosts economic grades of PGE (average grade of 3.8 ppm Pt+Pd+Rh+Au) over a lithological interval which may be up to 90 m thick (Grobler *et al.*, 2019). It was only recently discovered (Maier *et al.*, 2021), and development is under way to exploit this reef for PGE, Au, Ni, and Cu (Grobler *et al.*, 2019; McFall *et al.*, 2019).

The 'reef' portion of these rocks, representing the main target for exploitation of PGE and other metals, consists of sulphide-mineralized layers of dunite, harzburgite, and pyroxenite containing chromite stringers of no more than ca. 2 cm thick (Yudovskaya *et al.*, 2017; Grobler *et al.*, 2019). However, PGE mineralization associated with Ni– and Cu-bearing sulphides may extend below the reef for tens of metres into the footwall (Yudovskaya *et al.*, 2017; Grobler *et al.*, 2019). These rocks were emplaced upon the older Transvaal Supergroup sediments, and therefore they have a much greater degree of contamination (Keir-Sage *et al.*, 2021), though the Flatreef is generally considered to be less contaminated than the up-dip Platreef (Grobler *et al.*, 2019; Maier *et al.*, 2021).

Directly below the Flatreef, sporadic sulphide mineralization appears in a pile of rocks that may contain sedimentary xenoliths (Kinnaird and McDonald, 2005; Yudovskaya *et al.*, 2017; Grobler *et al.*, 2019). The original composition of these xenoliths ranges from carbonate (dolostone) to pelitic (shale) and quartzitic, and also includes evaporitic rocks (Hutchinson and Kinnaird, 2005; Grobler *et al.*, 2019). The rocks of this pile are layered and may be underlain by a chromitite seam recognized as correlating with the UG-2 elsewhere in the BC (Grobler *et al.*, 2019; Langa *et al.*, 2021). Where sedimentary xenoliths are not abundant, this zone is termed the Footwall Cyclic Unit (FCU) (Grobler *et al.*, 2019).

In the central region of the Flatreef Project area, the most sedimentary xenoliths may be found in the FCU (Yudovskaya *et al.*, 2017; Grobler *et al.*, 2019). In this region, the FCU is also more variable, consisting of abundant pegmatitic mafic and ultramafic rocks, and some rock types appear to have been altered (Grobler *et al.*, 2019). These rocks, where interaction of magma with sediment is highly evident, are termed the Footwall Assimilation Zone (FAZ) (Grobler *et al.*, 2019; Mayer *et al.*, 2021). Xenoliths found in this zone are often metamorphosed and recrystallized; for example, argillite is often altered to hornfels and dolostones or limestones form marble and localized skarn assemblages (Grobler *et al.*, 2019). Sporadic zones of pegmatoidal 'parapyroxenite' and serpentinized 'paraharzburgite' occur in these rocks (Yudovskaya *et al.*, 2017; Grobler *et al.*, 2019). They represent an alteration of the normal mafic-ultramafic assemblage, and may be interpreted as products of an ultramafic magma that was contaminated (with Ca originating from dolostone/ limestone) by the sediments, and crystallized in the presence of volatiles resulting from melting of sedimentary xenoliths (Grobler *et al.*, 2019).

Below the entire Flatreef sequence, sills of dunite, pyroxenite, and harzburgite may be found intruding the Transvaal Supergroup (Grobler *et al.*, 2019; Yudovskaya *et al.*, 2021). The package of rocks from the lower chromitite seam up to the noritic cyclic units above the Flatreef shows better mineral layering with less contamination than the Platreef, and can be well correlated with the interval from the UG-2 up to the Bastard Reef (above the Merensky Reef) in the western and eastern limbs of the BC (Grobler *et al.*, 2019; Beukes *et al.*, 2021; Mayer *et al.*, 2021).

In parts of the FAZ, as is evident from several exploration boreholes drilled by Ivanplats for the Flatreef Project, pegmatoidal clinopyroxenite is well developed over many metres of depth. This clinopyroxenite belongs to the parapyroxenite lithologies that have been affected by contamination with sedimentary material (Grobler *et al.*, 2019). It occurs close to the footwall of the Flatreef mineralized zone and therefore provides an important starting point when studying the Sc content of the BC, since this metal is almost always mined as a by-product to other commodities.

The purpose of this paper is not only to evaluate the scandium content of the Flatreef, but also to provide an overview of existing Sc data for the Critical Zone (CZ) of the Rustenburg Layered Suite of the BC. This is then compared to global deposits and the average Sc contents of mafic to ultramafic igneous rocks. The authors intend this paper to serve as a repository of knowledge as well as a discussion of possibilities pertaining to the economic potential of existing South African mineral ores.

Samples and methods

Samples analysed for scandium in this study include clinopyroxenites from the Flatreef (described below), as well as chromitite and associated silicate rocks (pyroxenite, norite, anorthosite) of the Critical Zone of the eastern BC (see Figure 1a). Preceding Sc analysis, major elements in all samples were analysed by XRF and the normative mineralogy was calculated. The eastern BC samples originate from borehole WV-30 drilled on the Winterveld property of Samancor's Eastern Chrome Mine. A thorough petrological and mineralogical overview of these samples, as well as their location relative to the eastern limb of the BC, is given in Kotzé and Gauert (2020). Figures 2a–d show typical mineral and textural characteristics of these samples. Sample WV52.1 (Figure 2b) represents the first anorthosite of the Critical Zone, which marks the start of the Upper Critical Zone (UCZ), which is defined by the presence of cumulus plagioclase (*e.g.* Kinnaird *et al.*, 2002). Sample WV-65 is a massive, nearly monomineralic chromitite with variable grain size from the LG-6, which is mined for Cr at Winterveld. All of the samples from the eastern Bushveld used in this study represent a relatively unaltered, nearly pristine magmatic assemblage that is likely representative of equivalent rocks throughout the eastern and

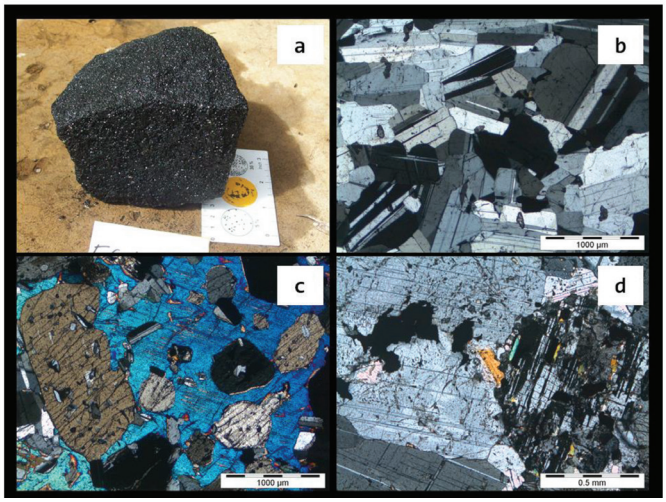

Figure 2—Textures of samples originating from the eastern limb of the BC. (a) Massive chromitite from the LG-3, once beneficiated for Cr. (b) Anorthosite just above the MG-2; first appearance of cumulus plagioclase in the Critical Zone. (c) Norite of the UCZ. Plagioclase and orthopyroxene (white and brown) are enclosed within a large clinopyroxene oikocryst (dark blue). (d) Rare example of hydrothermal alteration in the WV samples. Base metal sulphide, identified as pyrrhotite (black) occurs along a micro-vein in UCZ norite. Muscovite (pale pink) and biotite (orange) are associated with the sulphide. To the right (black), a large orthopyroxene grain is heavily altered. (b–d) Photomicrographs taken under cross-polarized (CPL), transmitted light

western limbs of the BC (Kotzé and Gauert, 2020). The most notable post-magmatic effects that were active with regard to these samples are those that occurred purely as a result of magmatic processes – for example, the scavenging of Fe from sulphide minerals by nonstochiometric chromite ($FeCr_2O_4$), leading to replacement of pyrrhotite by pyrite alongside sulphur loss from chromitite layers (Naldrett and Lehmann, 1988; Naldrett *et al.*, 2012), resulting in mobilization of S in late-stage magmatic fluids, which produced limited features of high-temperature hydrothermalism (Figure 2d) (Kanitpanyacharoen and Boudreau, 2013; Kotzé and Gauert, 2020).

One sample, LG306 (see Table II) originated from an abandoned pit on the Winterveld property. This sample represents the LG-3 chromitite layer, which was exploited for chromium at that site. This chromitite seam occurs at about 4 m depth below the surface in the eastern BC just north of the Steelpoort Fault. It is a massive, coarse-grained chromitite with very little interstitial material (Figure 2a).

Tables II–IV list the rock type of each sample as well as the name of the borehole and depth at which each sample was taken.

Flatreef samples

Samples from the Flatreef and associated rock units that were analysed for this study belong to four groups: the Flatreef itself, the FCU, the UG-2- equivalent chromitite seam, and finally the FAZ. All samples were taken from Ivanplats' UMT exploration boreholes, which are described in Grobler *et al.* (2019). The area of the northern limb where these boreholes were drilled is illustrated in Figure 1b. The borehole numbers may be found in Tables III and IV. Assays of Pt, Pd, Rh, Au, Cr, Ni, Cu, and S were provided by Ivanplats. The methodology for these analyses is described in Peters *et al.* (2017) and Grobler *et al.* (2019). The samples taken for this study are all mineralized with regard to PGE and the base metals, and all contain visible base metal sulphide (BMS).

Two samples were taken from the Flatreef itself, consisting respectively of harzburgite (M1-lower) and pyroxenite (pegmatoidal orthopyroxenite, M1-upper). These two samples were judged to be representative of typical lower reef facies as described in Yudovskaya *et al.* (2017) and Grobler *et al.* (2019). Both samples contain visible disseminated sulphide mineralization, with the main sulphide minerals being pentlandite, pyrrhotite, and chalcopyrite. The pyroxenite sample (KO32) contains abundant green clinopyroxene. The harzburgite sample (KO2) is relatively high-grade with total Pt+Pd+Rh+Au *ca.* 5.5 ppm. The pyroxenite, on the other hand, is of lower grade, with Pt+Pd+Rh+Au *ca.* 1 ppm. The pyroxenite also contains about 0.4 w% Cr, likely from minor chromite, but possibly also in clinopyroxene. The harzburgite contains only 540 ppm Cr. Textures and mineralogy of these two samples are depicted in Figure 3a–d. Notably, these samples are much more altered compared to the eastern limb samples, with abundant serpentinization of olivine (Figure 3a), and abundant biotite and chlorite. Plagioclase also displays alteration along microfractures, most likely to sericite (Figure 3b).

Two samples originated from the FCU just below the Flatreef. These consist of pyroxenite and norite, respectively. The pyroxenite (KO14) contains both ortho- and clinopyroxene, and hosts inclusions of what are probably sedimentary xenoliths. The norite sample (KO6) also contains abundant clinopyroxene, and has a pegmatitic texture. The norite contains relatively high-grade PGE mineralization (*ca.* 6 ppm Pt+Pd+Rh+Au) and abundant disseminated sulphide, whereas the pyroxenite is only sparsely mineralized with respect to BMS and contains slightly less than 0.5 ppm Pt+Pd+Rh+Au. Textures and mineralogy of these samples are depicted in Figures 4a–b. These footwall samples show greater alteration compared to the samples from the Flatreef. There are abundant masses of mica and clay, along with occasional crystal growth of secondary minerals. Both macroscopically and microscopically, the mineral grains display irregular, rounded edges, suggesting possible postmagmatic re-melting and alteration (Figures 4a).

Two samples were taken from the UG-2- equivalent chromitite seam below the Flatreef. Sample KO25-Cr represents the chromitite portion of the seam, and KO25-Px is a pegmatoidal pyroxenite very similar to the pyroxenite which underlies the UG-2 chromitite in the eastern and western limbs. The PGE content of both pyroxenite and chromitite together is given as around 3 ppm. Textures and mineralogy of these samples

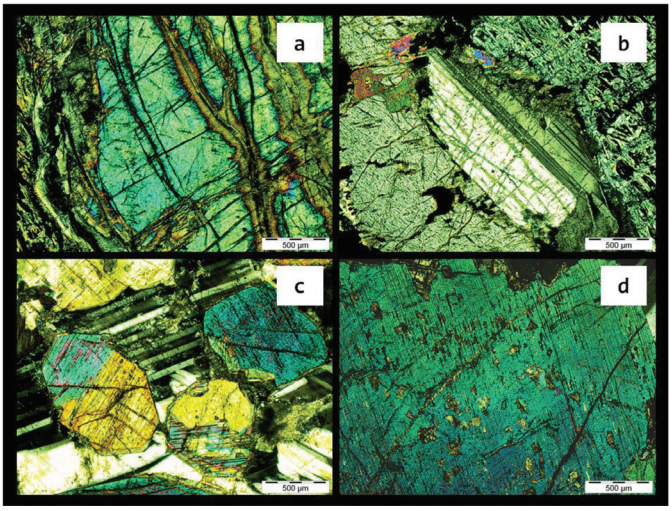

Figure 3—Mineralogical textures in the Flatreef. (a) Serpentinization of olivine (green) along fractures in harzburgite. (b) Plagioclase grain (black-and-white, centre) with sericitic alteration in harzburgite. In the bottom left corner is an orthopyroxene grain; in the top right, a mass of serpentine. The brightly coloured grains in the top left are biotite. (c)Clinopyroxene grains (bright blue and yellow) against interstitial plagioclase in pyroxenite. (d) Surface of a large clinopyroxene grain in pyroxenite showing abundant inclusions and infill of crystal fractures. All photomicrographs taken under crossed-polarized light (CPL)

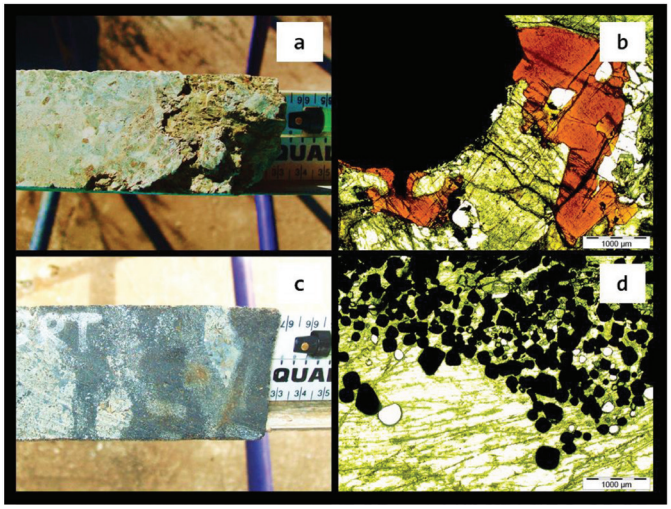

Figure 4—Mineralogical textures of the FCU and UG-2 equivalent chromitite. (a) Abundant green clinopyroxene, coarse-grained pegmatitic texture, and irregular grain edges in norite of the FCU. (b) Large round sulphide grain (black) associated with biotite (orange) and orthopyroxene (brown). (c) Chromitite showing disruption of the layers. (d) Microscopic texture of contact between chromitite and pyroxenite, showing orthopyroxene (brown) enclosing chromite grains (black). Similar chromitite textures are found in the eastern and western limbs. (b) and (d) are photomicrographs, taken under plane-polarized (PPL) transmitted light

are shown in Figures 4c–d. The degree of alteration of these samples is similar to those from the Flatreef, and is limited to the pyroxenite rather than the chromitite. Macroscopically, the chromitite appears to have been disturbed by the surrounding silicate layers; individual seams are broken and discontinuous (Figure 4c).

In total, seven samples from the FAZ were analysed. Samples KO33 to KO38 are well mineralized with respect to PGE, with total Pt+Pd+Rh+Au ranging from *ca.* 3 to *ca.* 7 ppm. Sample KO7 is exceptionally high grade, with Pt+Pd+Rh+Au just over 9 ppm. For these samples, sulphide-mineralized horizons with appreciable PGE content and abundant visible clinopyroxene were specifically targeted. Textures and mineralogy may be seen in Figures 5a–d. All samples consist of parapyroxenite, with textures similar to the irregular, rounded grain edges of lithologies in the FCU above (Figure 5a). However, in the FAZ, the grains appear much less well ordered. The pyroxenite is very coarse-grained, and contains abundant visible sulphide (Figure 5a). Also visible are veins infilled with quartz or calcite (Figure 5b). These are often associated with large clusters of sulphide. Microscopically, evidence of re-melted pyroxene grains can be seen (Figure 5d), as well as the typical micaceous alteration. In contrast to the Flatreef, where alteration occurs along mineral fractures, in the FAZ there is clear evidence of infilled veins (Figures 5b–c).

Sc analysis

All 22 samples were analysed at the University of the Free State, South Africa, on pressed powder pellets using a Rigaku ZSX Primus IV wavelength-dispersive X-ray fluorescence (XRF) spectrometer. A custom calibration method was set up using a

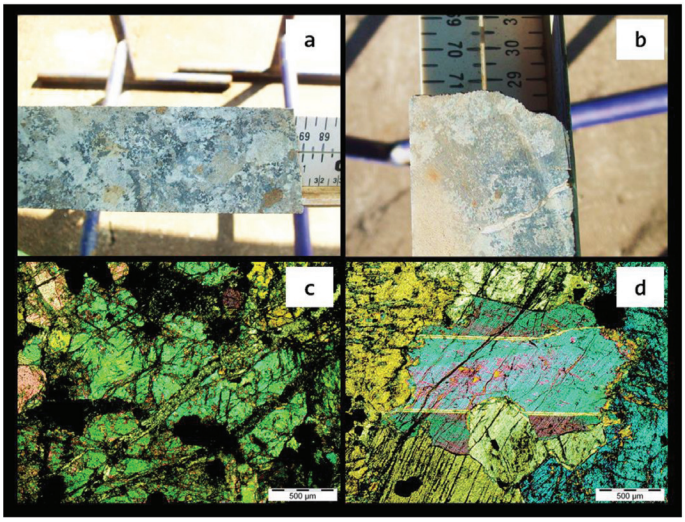

Figure 5—Textures and minerals of clinopyroxene-rich lithologies of the FAZ. (a) Parapyroxenite, showing rounded blebs of pyroxene. (b) Calcite vein cutting through parapyroxenite. (c) Vein infilled with chlorite, cutting across clinopyroxene grains. (d) Clinopyroxene grain (bright, middle of image) appears to have been partially dissolved and surrounded by a second-generation clinopyroxene grain. (c–d) Photomicrographs taken under cross-polarized light (CPL)

set of standards that covered the range of known rock types. The standard reference materials used consisted of SARM, GSJ, CCRM, and USGS rock powders of appropriate compositions. Standards with appropriate Sc values were tracked down by querying the GeoReM database by imputing the desired value ranges of Sc, as described by Jochum *et al.* (2005). The database provides measured values of any element, as well as recommended, compiled, and certified values. Because Sc has no certified value for any of the available standards, compiled Sc values from Govindaraju (1994) were used for each standard in the calibration after using GeoReM for lookup and reference. After the calibration was set up, each standard was analysed as a sample to test the precision of the calibration, which was found to be excellent (Table I). Duplicate samples were included in analytical runs to ensure accuracy, which was within acceptable limits (10%). The lower limit of detection was 2 ppm, and the lower limit of quantification was 3 ppm for Sc.

The analysed values for the Eastern Bushveld chromitites and associated lithologies can be found in Table II. The results for the Flatreef, UG-2 equivalent in the northern limb, and FCU samples are in Table III. Sc results for samples originating from the FAZ are in Table IV.

Table I

Sc contents (in ppm) of certified reference materials used for analysis

Standard name	Rock type	Compiled value* (Govindaraju, 1994)	Analysed value
BHVO-1	Basalt	31	30
JB-2	Basalt	54	54
JGb-1	Gabbro	36	36
MRG-1	Gabbro	54	53
SARM-4 (NIM-N)	Norite	38	37
SARM-5 (NIM-P)	Pyroxenite	29	30

Results and discussion

Sc in the Main and Critical Zones

Despite Sc being used as a trace element to track igneous processes such as fractional crystallization and partial melting, particularly in relation to vanadium, (Allègre *et al.*, 1977; Lee *et al.*, 2005), assay values for Sc in the BC are relatively sparse. No reference information can be found regarding concentrations in Sc in the Critical Zone of the RLS below the Merensky Reef, hence Sc concentrations of chromitites and associated lithologies that we present in this paper appear to be the first of their kind.

The concentration of Sc in the primitive mantle is calculated to be about 16.5 ppm (Lee *et al.*, 2005). In pyroxenitic igneous rocks, as has been discussed above, Sc may reach (sub-)economic concentrations of 50 ppm or above. Looking at the standard reference materials described in Govindaraju (1994), basalts and gabbros such as the USGS standard BHVO-1 and the CCRM standard MRG-1 typically contain about 20–50 ppm Sc (see Table I). Anorthositic rocks, however, do not preferentially concentrate Sc and have much lower concentrations (15 ppm or below) (see *e.g.* Mitchell 1986; Boudreau 2016).

One of the main sources for Sc concentrations in the Main Zone of the BC (above the level of the Bastard Reef) is Mitchell (1986), who found Sc concentrations to vary from 5 ppm (in anorthosite) to 40 ppm (in pyroxenite). Scandium was strongly correlated with clinopyroxene. Arndt *et al.* (2005) determined Sc along with other trace elements in the Merensky Reef unit and associated rocks. The concentration of Sc varied from 9 to 22 ppm, which is relatively low. Notably, the Merensky Reef samples in this study are mineralogically dominated by orthopyroxene and plagioclase, with almost no clinopyroxene.

The Lower Main Zone and Platreef of the northern limb (Roelofse and Ashwal, 2012) show a slightly higher average, with Sc ranging from 20–36 ppm in gabbroic and noritic lithologies, excluding outliers. Anorthosite and leuconorite, as expected, have lower concentrations (10–18 ppm Sc).

The analysed values of Sc presented in Table II closely approximate the exact ranges in the Main Zone, Merensky Reef, and Platreef as discussed above, with maximum concentrations ranging above the Merensky Sc concentrations as given by Arndt *et al.* (2005). The two massive chromitites from the LG-6

Table II

Samples analysed for Sc from the chromitites of the eastern limb of the Bushveld Complex

Location	Borehole	Lithology	Depth(m)	Sample no.	Sc(ppm)
Eastern Bushveld chromitites					
Upper CZ (UG1-FW)	WV30	Leuconorite Pyroxenite (Fs)	336.25 - 336.41 353 - 353.2	WV28A WV29	14 32
MG-5	WV30	Cr-melanorite Melanorite	371.85 - 371.95 382.8 - 383	WV30 WV34	6 40
Upper CZ (MG5-FW)	WV30	Melanorite	413 - 413.2	WV35	27
Upper CZ (MG2-HW)	WV30	Anorthosite (1st)	538.44 - 538.57	WV52.1	<3
LG-6	WV30	Chromitite	599.14 - 599.24	WV65	<3
Lower CZ (LG6-FW)	WV30	Pyroxenite	643 - 643.2	WV62	19
LG-3	Pit	Chromitite	4	LG306	<3

LLD = 2ppm; LOQ = 3ppm. cpx = clinopyroxenite. peg = pegmatoidal. Fs = feldspathic. CZ = Critical Zone. FW = footwall. HW = hanging wall. 1st = first cumulus plagioclase. LG, MG, UG = Lower, Middle, Upper Group (chromitite)

Table III

Samples analysed for Sc from the Flatreef and associated lithologies

Location	Borehole	Lithology	Depth(m)	Sample no.	Sc(ppm)
Flatreef (Merensky Reef correlate)					
Flatreef	UMT263	Harzburgite	851 - 851.31	KO2	8
	UMT397	Orthopyroxenite (peg)	947.4 - 947.66	KO32	40
Footwall Cyclic Unit					
Flatreef	UMT276	Pyroxenite	817 - 817.18	KO14	36
	UMT263	Norite	879 - 879.15	KO6	20
Cr seam (UG-2 correlate)					
Flatreef	UMT345	Pyroxenite (peg)	1519.98 - 1520.11	KO25-Px	30
		Chromitite	1520.11 - 1520.26	KO25-Cr	12

LLD = 2ppm; LOQ = 3ppm. cpx = clinopyroxenite. peg = pegmatoidal. Fs = feldspathic. CZ = Critical Zone. FW = footwall. HW = hanging wall. 1st = first cumulus plagioclase. LG, MG, UG = Lower, Middle, Upper Group (chromitite)

Table IV

Samples analysed for Sc from the Footwall Assimilation Zone below the Flatreef

Location	Borehole	Lithology	Depth(m)	Sample no.	Sc(ppm)
Footwall Assimilated Zone					
Flatreef	UMT319	Parapyroxenite (px)	879.08 - 879.34 880.11 - 880. 31 880.67 - 880.83	KO33 KO34 KO35	10 21 23
Flatreef	UMT263 UMT332	Parapyroxenite	910.43 - 910.64 1164.19 - 1164.35	KO7 KO36	13 7
Flatreef	UMT331	Parapyroxenite	1176.31 - 1176.58 1176.83 - 1176.96	KO37 KO38	23 28

LLD = 2ppm; LOQ = 3ppm. cpx = clinopyroxenite. peg = pegmatoidal. Fs = feldspathic. CZ = Critical Zone. FW = footwall. HW=hanging wall. 1st = first cumulus plagioclase. LG, MG, UG = Lower, Middle, Upper Group (chromitite)

and LG-3, as well as the only anorthosite sample, contain Sc concentrations below the limit of quantification. Considering the rest of the results, this is clearly due to the fact that these horizons contain almost no pyroxene – all three of these samples can be said to be monomineralic, with the chromitites strongly excluding any mineral but chromite, and the anorthosite with only Ca-plagioclase and no visible pyroxene. Sc consistently correlates with rock type, with the melanorites and pyroxenites ranging from about 20 to 40 ppm, while anorthosite and leuconorite have concentrations below 20 ppm. Variations between individual layers may simply be due to the amount of clinopyroxene *versus* orthopyroxene. In the Lower Critical Zone (LCZ), orthopyroxene is the most important cumulus phase, and correspondingly the LCZ pyroxenite (WV62) in Table II has Sc of just below 20 ppm. The very low Sc content in the chromitiferous melanorite of the MG-5 (sample WV30; 6 ppm) can be explained by the high concentration of Cr_2O_3 (40%) in this sample, indicating high chromite content, in addition to the fact that it contains mainly orthopyroxene rather than clinopyroxene. These results agree with the theory that Sc preferentially associates with clinopyroxene above all other minerals. Based on these results, Sc does not appear to be compatible with chromite.

Sc in the Flatreef

The values from the Flatreef, UG-2- equivalent and FCU shown in Table III correspond to the ranges in the previous results. Again, Sc correlates closely to rock type, with olivine-rich harzburgite of the Flatreef showing low values (8 ppm) and the clinopyroxene-rich pyroxenites of the reef and footwall with higher values (up to 40 ppm). The analysed value for pyroxenite associated with the UG-2 fits in with values found for pyroxenite of the Critical Zone in the eastern limb.

Values of Sc found in the FAZ fit into the ranges for the BC discussed so far, but interestingly, despite clinopyroxene-rich lithologies being targeted for analysis, including two samples (KO34 and KO35) with an estimated 71–73% modal clinopyroxene, the values actually trend lower than those found in the unaltered eastern limb and the relatively unaltered Flatreef, with the lowest value being 9 ppm and the highest 28 ppm. This may be a sign that the extensive alteration found in the FAZ might have redistributed scandium that was originally concentrated in the clinopyroxenes. Alteration of clinopyroxene to mica would mean that Sc, incompatible in the crystal structure of mica, might partition into a hydrothermal fluid. If so, the eventual fate of the Sc is still unknown, since no likely reservoirs have been found in the BC.

The presence of clinopyroxene-rich parapyroxenite in the FAZ has been interpreted to represent a recrystallization of originally igneous cumulates in the presence of a Ca-rich fluid originating from crustal sediments of carbonatic composition (Grobler *et al.*, 2019). During this process, trace elements from crustal material must also have been introduced into the Bushveld cumulates. Scandium does not appear to have been introduced from the crust, nor is this likely, since Sc tends to be strongly associated with igneous processes (Williams-Jones and Vasyukova, 2018; Wang *et al.*, 2021).

Figure 6 illustrates the ranges of Sc for different zones of the BC, as found in this study and taken from literary sources. Sc values overlap for the Main Zone of both the northern and western limbs. Values of Sc for the Flatreef reef portions, the FCU, and the Critical Zone of the eastern limb in this study largely fit within the same parameters, with Sc generally increasing with the amount of clinopyoroxene. There also appears to be a steep trend of Sc enrichment in a few samples including silicate and chromitite samples from the Critical Zone as well as the Flatreef pegmatoidal pyroxenite, two FAZ samples, and a few Main Zone samples. A possible explanation for this 'trend' is that these samples were trapped between other layers (for example, silicate inclusions in chromitite layers) and thus Sc could not concentrate as efficiently into the clinopyroxene fraction.

Most of the FAZ samples analysed in this study plot along a gentle trend of Sc enrichment with increasing clinopyroxene (see Figure 6). The deficiency in Sc for the FAZ, as discussed above can clearly be seen in this graph.

Certainly, the values of Sc that we have found in the BC for this study do not appear to be economic, even if Sc were to be exploited as a by-product. With improving recovery through enhanced leaching processes and increasing demand for Sc leading to rising prices, this could conceivably change. The Southern African mining industry thrives on innovation; selenium and tellurium, two other metals associated with growing technologies, are now being produced from copper refinery anode slimes in Ndola, Zambia (Dworzanowski, 2019). Even the low grades of Sc found in this study can be of economic interest, especially considering that the Sc 'missing' from the FAZ may be concentrated elsewhere.

Concluding remarks

The values of Sc in the Bushveld Complex strongly correlate with the presence of clinopyroxene and do not differ significantly from Sc concentrations for typical mafic-ultramafic rocks, even in the lithologies of the northern limb, which are significantly contaminated with crustal material. The pyroxenites of the Critical Zone from the eastern limb and the Flatreef of the northern limb from this study contain approximately 40 ppm Sc, whereas the Merensky pyroxenite of the eastern and western limbs contains about 22 ppm Sc on average. The difference is most likely due to the increasing cpx to opx ratio, which corresponds with higher cpx concentrations in the CZ and the Flatreef lithologies.

Acknowledgments

The authors wish to thank the staff of Ivanplats in Mokopane, particularly Mr Fabian Fredericks, for their kind co-operation in obtaining sample material and previous assays for this study, as well as assistance in understanding the lithologies of the Flatreef. This research was entirely supported by post-doctoral funding from the University of the Free State.

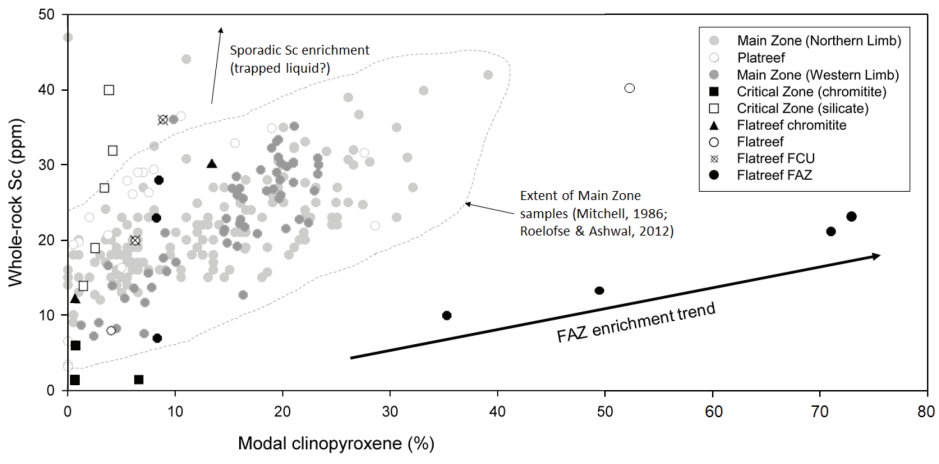

Figure 6—Values of Sc against modal clinopyroxene for the Main Zone of the western limb (Mitchell, 1986) and northern limb (Roelofse and Ashwal, 2012), the Critical Zone of the eastern limb (this study), and different lithologies of the Flatreef (this study)

References

Allègre, C., Treuil, M., Minster, J.-F., Minster, B., and Albarède, F. 1977. Systematic use of trace element in igneous process Part I: Fractional crystallization processes in volcanic suites. *Contributions to Mineralogy & Petrology*, vol. 60. pp. 57–75. https://doi.org/10.1007/BF00372851

Arndt, N., Jenner, G., Ohnenstetter, M., Deloule, E., and Wilson, A. 2005. Trace elements in the Merensky Reef and adjacent norites Bushveld Complex South Africa. *Mineralium Deposita*, vol. 40. pp. 550–575. https://doi.org/10.1007/s00126-005-0030-x

Beukes, J., Roelofse, F., Gauert, C., Grobler, D., and Ueckermann, H. 2021. Strontium isotope variations in the Flatreef on Macalacaskop, northern limb, Bushveld Complex: Implications for the source of platinum-group elements in the Merensky Reef. *Mineralium Deposita*, vol. 56. pp. 45–57. https://doi.org/10.1007/s00126-020-00998-2

Boudreau, A. 2016. The Stillwater Complex, Montana – Overview and the significance of volatiles. *Mineralogical Magazine*, vol. 80, no. 4. pp. 585–637. https://doi.org/10.1180/minmag.2016.080.063

Burke, S. 2022. Opinion: Russia is a mineral powerhouse – and its war with Ukraine could affect global supplies. https://www.bostonglobe.com/2022/03/09/opinion/russia-is-mineral-powerhouse-its-war-with-ukraine-could-affect-global-supplies [accessed 9 May 2022].

Cameron, E. and Desborough, G. 1966. Occurence and characteristics of chromite deposits – Eastern Bushveld Complex. *Magmatic Ore Deposits: A Symposium*. Wilson (ed.). Economic Geology Publishing Company. pp. 23–40.

Cawthorn, R., Eales, H., Walraven, F., Uken, R., and Watkeys, M. 2006. The Bushveld Complex. *The Geology of South Africa*. Johnson, M., Anhaeusser, C., Thomas, R. (eds.)Geological Society of South Africa, Johannesburg/Council for Geoscience, Pretoria. pp. 261–281.

Cawthorn, R., Lee, C., Schouwstra, R., and Mellowship, P. 2002. Relationship between PGE and PGM in the Bushveld Complex. *Canadian Mineralogist*, vol. 40. pp. 311–328. https://doi.org/10.2113/gscanmin.40.2.311

Cawthorn, R. and Webb, S. 2001. Connectivity between the western and eastern limbs of the Bushveld Complex. *Tectonophysics*, vol. 330. pp. 195–209. https://doi.org/10.1016/S0040-1951(00)00227-4

Coetzee, J. and Twist, D. 1989. Disseminated tin mineralization in the roof of the Bushveld granite pluton at the Zaaiplaats Mine, with Implications for the genesis of magmatic hydrothermal tin systems. *Economic Geology*, vol. 84. pp. 1817–1834. https://doi.org/10.2113/gsecongeo.84.7.1817

Cousins, C. 1966. The Merensky Reef of the Bushveld Igneous Complex. *Magmatic Ore Deposits: A Symposium*. Wilson, H.D. (ed.). Economic Geology Publishing Company. pp. 239–251.

Cramer, L. 2001. The extractive metallurgy of South Africa's platinum ores. *Journal of The Minerals, Metals & Materials Society*, vol. 53. pp. 14–18. https://doi.org/10.1007/s11837-001-0048-1

Deer, W., Howie, R., and Zussman, J. 2013. Chain silicates. *Deer, W., Howie, R. & Zussman, J. An Introduction to the Rock-Forming Minerals*, 3rd edn. The Mineralogical Society, London. pp. 94–131.

Dworzanowski, M. 2019. Base metals production in Southern Africa provides the common thread between all the country branches in the SAIMM. *Journal of the Southern African Institute of Mining and Metallurgy*, vol. 119. pp. 50–51.

European Commission. 2020. Critical raw Mmaterials resilience: Charting a path towards greater security and sustainability. Communication from the Commission to the European Parliament, the Council, the European Economic and Social Committee and the Committee of the Regions, Brussels. https://eur-lex.europa.eu/legal-content/EN/ALL/?uri=COM:2020:474:FIN [accessed 5 November 2021].

Godel, B., Barnes, S.-J., and Maier, W. 2007. Platinum-group elements in sulphide minerals, platinum-group minerals, and whole-rocks of the Merensky Reef (Bushveld Complex, South Africa): Implications for the formation of the Reef. *Journal of Petrology*, vol. 48, no. 8. pp. 1569–1604. https://doi.org/10.1093/petrology/egm030

Govindaraju, K. 1994. Compilation of working values and sample description for 383 geostandards. *Geostandards Newsletter*, vol. 18. pp. 1–158. https://doi.org/10.1046/j.1365-2494.1998.53202081.x-i1

Grobler, D., Brits, J., Maier, W., and Crossingham, A. 2019. Litho– and chemostratigraphy of the Flatreef PGE deposit, northern Bushveld Complex. *Mineralium Deposita*, vol. 54. pp. 3–28. https://doi.org/10.1007/s00126-018-0800-x

Harmer, R. and Sharpe, M. 1985. Field relations and strontium isotope systematics of the marginal rocks of the eastern Bushveld Complex. *Economic Geology*, vol. 80. pp. 813–837. https://doi.org/10.2113/gsecongeo.80.4.813

Harney, D. and Von Gruenewaldt, G. 1995. Ore-forming processes in the upper part of the Bushveld Complex, South Africa. *Journal of African Earth Sciences*, vol. 20, no. 2. pp. 77–89. https://doi.org/10.1016/0899-5362(95)00034-Q

Hawthorne, F. and Grundy, H. 1973. Refinement of the crystal structure of $NaScSi_2O_6$. *Acta Crystallographica Section B, Structural Science*, vol. 29, no. 11. pp. 2615–2616. https://doi.org/10.1107/S0567740873007156

Hughes, H., Andersen, J., and O'Driscoll, B. 2020. Mineralization in layered mafic-ultramafic intrusions. *Encyclopedia of Geology*. 2nd edn. Alderton. D. & Elias, S. (eds.). Academic Press. pp. 823–839. https://doi.org/10.1016/B978-0-08-102908-4.00037-0

Hutchinson, D. and Kinnaird, J. 2005. Complex multistage genesis of the Ni-Cu-PGE mineralisation in the southern region of the Platreef, Bushveld Complex, South Africa. *Transactions of the Institution of Mining and Metallurgy, Section B: Applied Earth Sciences*, vol. 114, no. 4. pp. 208–224. https://doi.org/10.1179/037174505X82125

Jochum, K., Nohl, U., Herwig, K., Lammel, E., Stoll, B., and Hofmann, A. 2005. GeoReM: A new geochemical database for reference materials and isotopic standards. *Geostandards and Geoanalytical Research*, vol. 29, no. 3. pp. 333–338. https://doi.org/10.1111/j.1751-908X.2005.tb00904.x

Jacobs, M. 2006. Process description and abbreviated history of Anglo Platinum's Waterval Smelter. *Proceedings of Pyrometallurgy 2006*, Cradle of Humankind, South Africa, 5-8 March 2006. Jones, R. (ed.) Southern African Institute of Mining and Metallurgy, Johannesburg. pp. 17–28.

Johnston, R. 2022. Supply of critical minerals amid the Russia-Ukraine war and possible sanctions. Columbia University SIPA Center on Global Energy Policy. https://www.energypolicy.columbia.edu/research/commentary/supply-critical-minerals-amid-russia-ukraine-war-and-possible-sanctions

Jones, R. 2005. An overview of Southern African PGM smelting. *Proceedings of Nickel and Cobalt 2005: Challenges in Extraction and Production, The 44th Annual Conference of Metallurgists*, Calgary, Alberta, Canada, 21-24 August 2005. Schonewille, R. and Donald, J. (eds.) Canadian Institute of Mining, Metallurgy and Petroleum, Montreal. pp. 147–178.

Kahn, J. 2022. The chip shortage crippled parts of the world economy. A Russian invasion of Ukraine would make it even worse. https://fortune.com/2022/02/14/russia-ukraine-semiconductor-shortage/ [accessed 9 May 2022].

Kanitpanyacharoen, W. and Boudreau, A. 2013. Sulfide-associated mineral assemblages in the Bushveld Complex, South Africa: Platinum-group element enrichment by vapor refining by chloride–carbonate fluids. *Mineralium Deposita*, vol. 48. pp. 193–210. https://doi.org/10.1007/s00126-012-0427-2

Keir-Sage, E., Leybourne, M., Jugo, P., Grobler, D., and Mayer, C. 2021. Assessing the extent of local crust assimilation within the Flatreef, northern limb of the Bushveld Igneous Complex, using sulfur isotopes and trace element geochemistry. *Mineralium Deposita*, vol. 56. pp. 91–102. https://doi.org/10.1007/s00126-020-01024-1

Kinnaird, J., Hutchinson, D., Schurmann, L., Nex, P., and De Lange, R. 2005. Petrology and mineralisation of the southern Platreef: northern limb of the Bushveld Complex, South Africa. *Mineralium Deposita*, vol. 40. pp. 576–597. https://doi.org/10.1007/s00126-005-0023-9

Kinnaird, J., Kruger, F., Nex, P., and Cawthorn, R. 2002. Chromitite formation – A key to understanding processes of platinum enrichment. *Transactions of the Institution of Mining and Metallurgy, Section B: Applied Earth Sciences*, vol. 111, no. 1. pp. 23–35. https://doi.org/10.1179/aes.2002.111.1.23

Kinnaird, J. and McDonald, I. 2005. An introduction to mineralisation in the northern limb of the Bushveld Complex. *Transaction of the Institute of Mining and Metallurgy: Section B. Applied Earth Sciences*, vol. 114, no. 4. pp. 194–198. https://doi.org/10.1179/037174505X62893

Kotzé, E. and Gauert, C. 2020. PGE distribution in the chromitite layers at Eastern Chrome Mine, Eastern Bushveld Complex, South Africa: A descriptive study with comparison of EPMA and LA-ICP-MS methods for detection of trace PGE in base metal sulphides. *South African Journal of Geology*, vol. 123, no. 4. pp. 551–572. https://doi.org/10.25131/sajg.123.0033

Kruger, F. 2005. Filling the Bushveld Complex magma chamber: Lateral expansion, roof and floor interaction, magmatic unconformities, and the formation of giant chromitite, PGE and Ti-V-magnetitite deposits. *Mineralium Deposita*, vol. 40. pp. 451–472. https://doi.org/10.1007/s00126-005-0016-8

Langa, M., Jugo, P., Leybourne, M., Grobler, D., Adetunji, J., and Skogby, H. 2021. Chromite chemistry of a massive chromitite seam in the northern limb of the Bushveld Igneous Complex, South Africa: Correlation with the UG-2 in the eastern and western limbs and evidence of variable assimilation of footwall rocks. *Mineralium Deposita*, vol. 56. pp. 31–44. https://doi.org/10.1007/s00126-020-00964-y

Lee, C.-T., Leeman, W., Canil, D., and Li, Z.-X. 2005. Similar V/Sc systematics in MORB and arc basalts: Implications for the oxygen fugacities of their mantle source regions. *Journal of Petrology*, vol. 46, no. 11. pp. 2313–2336. https://doi.org/10.1093/petrology/egi056

Lee, C. 1996. A Review of mineralization in the Bushveld Complex and some other layered intrusions. *Developments in Petrology*. Cawthorn, R. (ed.). Elsevier. pp. 103–145. https://doi.org/10.1016/S0167-2894(96)80006-6

Lee, C. and Parry, S. 1988. Platinum-group element geochemistry of the Lower and Middle Group chromitites of the Eastern Bushveld Complex. *Economic Geology*, vol. 83. pp. 1127–1139. https://doi.org/10.2113/gsecongeo.83.6.1127

Maier, W., Abernethy, K., Grobler, D, and Moorhead, G. 2021. Formation of the Flatreef deposit, northern Bushveld, by hydrodynamic and hydromagmatic processes. *Mineralium Deposita*, vol. 56. pp. 11–30. https://doi.org/10.1007/s00126-020-00987-5

Maier, W., Yudovskaya, M., and Jugo, P. 2021. Introduction to the special issue on the Flatreef PGE-Ni-Cu deposit, northern limb of the Bushveld Igneous Complex. *Mineralium Deposita*, vol. 56. pp. 1–10. https://doi.org/10.1007/s00126-020-01027-y

Mayer, C., Jugo, P., Leybourne, M., Grobler, D., and Voinot, A. 2021. Strontium isotope stratigraphy through the Flatreef PGE-Ni-Cu mineralization at Turfspruit, northern limb of the Bushveld Igneous Complex: evidence of correlation with the Merensky Unit of the eastern and western limbs. *Mineralium Deposita*, vol. 56. pp. 59–72. https://doi.org/10.1007/s00126-020-01006-3

McFall, K., McDonald, I., Tanner, D., and Harmer, R. 2019. The mineralogy and mineral associations of platinum-group elements and precious metals in the Aurora Cu-Ni-Au-PGE deposit, Northern Limb, Bushveld Complex. *Ore Geology Reviews*, vol. 106. pp. 403–422. https://doi.org/10.1016/j.oregeorev.2019.02.008

Minh, N. 2004. Solid oxide fuel cell technology – Features and applications. *Solid State Ionics*, vol. 174. pp. 271–277. https://doi.org/10.1016/j.ssi.2004.07.042

Mitchell, A. 1986. The Petrology, Mineralogy and Geochemistry of the Main Zone of the Bushveld Complex at Rustenburg Platinum Mines, Union Section. PhD thesis, Rhodes University, Grahamstown, South Africa.

Morimoto, N., Fabries, J., Ferguson, A., Ginzburg, I., Ross, M., Seifert, F., Zussman, J., Aoki, K., and Gottardi, G. 1988. Nomenclature of pyroxenes. *American Mineralogist*, vol. 73. pp. 1123–1133. https://doi.org/10.1007/BF01226262

Naldrett, A. and Lehmann, J. 1988. Spinel non-stoichiometry as the explanation for Ni–, Cu– and PGE-enriched sulphides in chromitites. Prichard, H., Potts, P., Bowles, J. and Cribb S. (eds.). *Proceedings of Geo-Platinum*, vol. 87. pp. 93–109. Springer. https://doi.org/10.1007/978-94-009-1353-0_10

Naldrett, A., Wilson, A., Kinnaird, J., Yudovskaya, M., and Chunnett, G. 2012. The origin of chromitites and related PGE mienralization in the Bushveld Complex: New mineralogical and petrological constraints. *Mineralium Deposita*, vol. 47. pp. 209–232. https://doi.org/10.1007/s00126-011-0366-3

Nielsen, R., Gallaham, W., and Newberger, F. 1992. Experimentally determined mineral-melt partition coefficients for Sc, Y and REE for olivine, orthopyroxene, pigeonite, magnetite and ilmenite. *Contributions to Mineralogy and Petrology*, vol. 110. pp. 488–499. https://doi.org/10.1007/BF00344083

Oberthür, T., Junge, M., Rudashevsky, N., De Meyer, E., and Gutter, P. 2015. Platinum-group minerals in the LG and MG chromitites of the eastern Bushveld Complex, South Africa. *Mineralium Deposita*, vol. 51. pp. 71–87. https://doi.org/10.1007/s00126-015-0593-0

Peters, B., Parker, H., Joughin, W., Treen, J., Coetzee, V., and Marais, F. 2017. Platreef Project. Platreef 2017 Feasibility Study. https://ivanhoemines.com/site/assets/files/2981/platreef-feasibility-study-september-2017.pdf

Roelofse, F. and Ashwal, L. 2012. The Lower Main Zone in the northern limb of the Bushveld Complex—A >1.3 km thick sequence of intruded and variably contaminated crystal mushes. *Journal of Petrology*, vol. 53, no. 7. pp. 1449–1476. https://doi.org/10.1093/petrology/egs022

Scoon, R. and Mitchell, A. 1994. Discordant iron-rich ultramafic pegmatites in the Bushveld Complex and their relationship to iron-rich intercumulus and residual liquids. *Journal of Petrology*, vol. 35, no. 4. pp. 881–917. https://doi.org/10.1093/petrology/35.4.881

Scoon, R. and Mitchell, A. 2004. Petrogenesis of discordant magnesian dunite pipes from the central sector of the eastern Bushveld Complex with emphasis on the Winnaarshoek Pipe and disruption of the Merensky Reef. *Economic Geology*. vol. 99. pp. 517–541. https://doi.org/10.2113/gsecongeo.99.3.517

Shanghai Metals Market. 2022. *Daily metals price at metal.com.* (ccessed 29 May 2022).

SRK Consulting. 2018. Sunrise Nickel Cobalt Project, New South Wales, Australia. NI 43-101 Technical Report. https://www.miningnewsfeed.com/reports/Sunrise_Technical_Report_2018.pdf

Tarkian, M. and Stumpfl, E. 1975. Platinum mineralogy of the Driekop Mine, South Africa. *Mineralium Deposita* vol. 10, pp. 71–85. https://doi.org/10.1007/BF00207462

Taylor, C., Schulz, K., Doebrich, J., Orris, G., Denning, P., and Kirschbaum, M. 2005. Geology and nonfuel mineral deposits of Africa and the Middle East. *USGS Open-File Report* 2005-1294-E.

Teigler, B. and Eales, H. 1993. Correlation between chromite composition and PGE mineralization in the Critical Zone of the western Bushveld Complex. *Mineralium Deposita*, vol. 28. pp. 291–302. https://doi.org/10.1007/BF02739368

Teitler, Y., Cathelineau, M., Ulrich, M., Ambrosi, J, Munoz, M., and Sevin, B. 2019. Petrology and geochemistry of scandium in New Caledonian Ni-Co laterites. *Journal of Geochemical Exploration*, vol. 196. pp. 131–155. https://doi.org/10.1016/j.gexplo.2018.10.009

Van der Merwe, F., Viljoen, F., and Knoper, M. 2012. The mineralogy and mineral associations of platinum group elements and gold in the Platreef at Zwartfontein, Akanani Project, Northern Bushveld Complex, South Africa. *Mineralogy and Petrology*, vol. 106. pp. 25–38. https://doi.org/10.1007/s00710-012-0225-7

Van Tongeren, J., Mathez, E., and Kelemen, P. 2010. A felsic end to Bushveld differentiation. *Journal of Petrology*, vol. 51, no. 9. pp. 1891–1912. https://doi.org/10.1093/petrology/egq042

Viljoen, M. and Scoon, R. 1985. The distribution and main geologic features of discordant bodies of iron-rich ultramafic pegmatite in the Bushveld Complex. *Economic Geology*, vol. 80. pp. 1109–1128. https://doi.org/10.2113/gsecongeo.80.4.1109

Von Gruenewaldt, G., Hatton, C., and Merkle, R. 1986. Platinum-group element – chromitite associations in the Bushveld Complex. *Economic Geology*, vol. 81. pp. 1067–1079. https://doi.org/10.2113/gsecongeo.81.5.1067

Von Gruenewaldt, G., Sharpe, M., and Hatton, C. 1985. The Bushveld Complex: Introduction and Review. *Economic Geology*, vol. 80. pp. 803–812. https://doi.org/10.2113/gsecongeo.80.4.803

Von Gruenewaldt, G. and Strydom, J. 1985. Geochemical distribution patterns surrounding tin-bearing pipes and the origin of the mineralizing fluids at the Zaaiplaats Tin Mine, Potgietersrus District. *Economic Geology*, vol. 80. pp. 1201–1211. https://doi.org/10.2113/gsecongeo.80.4.1201

Voordouw, R. and Beukes, N. 2009. Alteration and metasomatism of the UG2 melanorite and its stratiform pegmatoids, Bushveld Complex, South Africa – Characteristics, timing and origins. *South African Journal of Geology*, vol. 112. pp. 47–64. https://doi.org/10.2113/gssajg.112.1.47

Wang, Z., Li, M., Liu, Z.-R., and Zhou, M.-F. 2021. Scandium: Ore deposits, the pivotal role of magmatic enrichment and future exploration. *Ore Geology Reviews*, vol. 128. p. 103906. https://doi.org/10.1016/j.oregeorev.2020.103906

Willemse, J. 1966. The geology of the Bushveld Igneous Complex, the largest repository of magmatic ore deposits in the world. *Magmatic Ore Deposits: A Symposium*. Wilson, H.D. (ed.). Economic Geology Publishing Company. pp. 1–22.

Williams-Jones, A. and Vasyukova, O. 2018. The Economic Geology of Scandium, the Runt of the Rare Earth Element Litter. *Economic Geology*, vol. 113, no. 4. pp. 973–988. https://doi.org/10.5382/econgeo.2018.4579

Xiao, J., Peng, Y., Ding, W., Chen, T., Zou, K., and Wang, Z. 2020. Recovering scandium from scandium rough concentrate using roasting-hydrolysis-leaching process. *Processes*, vol. 8. pp. 365. https://doi.org/10.3390/pr8030365

Xie, F., Zhang, T., Dreisinger, D., and Doyle, F. 2014. A critical review on solvent extraction of rare earths from aqueous solutions. *Minerals Engineering*, vol. 56. pp. 10–28. https://doi.org/10.1016/j.mineng.2013.10.021

Yudovskaya, M., Costin, G., Sluzhenikin, S., Kinnaird, J., Ueckermann, H., Abramova, V., and Grobler, D. 2021. Hybrid norite and the fate of argillaceous to anhydritic shales assimilated by Bushveld melts. *Mineralium Deposita*, vol. 56. pp. 73–90. https://doi.org/10.1007/s00126-020-00978-6

Yudovskaya, M., Kinnaird, J., Grobler, D., Costin, G., Abramova, V., Dunnett, T., and Barnes, S.-J. 2017. Zonation of Merensky-style platinum-group element mineralization in Turfspruit thick reef facies (Northern Limb of the Bushveld Complex). *Economic Geology*, vol. 112. pp. 1333–1365. https://doi.org/10.5382/econgeo.2017.4512

Zeh, A., Ovtcharova, M., Wilson, A., and Schaltegger, U. 2015. The Bushveld Complex was emplaced and cooled in less than one million years – results of zirconology, and geotectonic implications. *Earth and Planetary Science Letters*. vol. 418. pp. 103–114. https://doi.org/10.1016/j.epsl.2015.02.035 ◆